

Investigation of sintering of spherical copper powder by micro focus computed tomography (μ CT) and synchrotron tomography

M. Nöthe^{1,a}, M. Schulze^{2,b}, R. Grupp^{1,c}, B. Kieback^{1,d} and A. Haibel^{3,e}

¹Institute of Material Science, Technische Universität Dresden, Germany

²Institute of Photogrammetry and Remote Sensing, Technische Universität Dresden, Germany

³Structural Research, Hahn-Meitner-Institut Berlin, Germany

^amichael.noethe@tu-dresden.de, ^bmatthias.schulze@tu-dresden.de, ^crainer.grupp@hmi.de,

^dbernd.kieback@ifam-dd.fraunhofer.de, ^ehaibel@hmi.de

Keywords: Sintering, cooperative material transport, tomography, image analysing

Abstract. The two-particle model describes the approach of particle centres and the growth of the interparticle contacts during sintering of metal powders. Unfortunately the comprehensive description of processes inside of three dimensional specimens must consider the contribution of particle rearrangements. The recent developments of combined micro focus computed tomography (μ CT) and 3D photogrammetric image analyzing give the opportunity to obtain the experimental data required to overcome the shortcomings of sintering theories based on the two-particle model. The analysis of spherical poly and single crystalline copper powder was performed by μ CT. In addition a single crystal specimen was analyzed by high resolution synchrotron radiation tomography - a more sophisticated analysis method with very limited availability. The analysis of the 3D tomographic image by photogrammetric image analyzing yielded the positions and radii of all particles and their contact partners as well. A statistical analysis of the retrieved data was performed. The formation and breaking of necks during sintering could be observed. An in-depth analysis of the particle rotation with respect to the coordination number and local density will be presented.

Introduction

The well known two - particle model is the basic foundation of most theories of sintering processes. This model is well suited to describe the interparticle contact growth under the influence of the Laplace pressure. In this model the material transport by diffusion leads to the particle centre approach [1, 2, 3]. If no additional mass transport processes occur the theoretically deduced particle centre approach matches the shrinkage of the specimen [4]. Unfortunately real samples often show deviating shrinkage behaviour. This inconsistency is to be attributed to cooperative material transport mechanisms for example the rearrangement of particles by rotations [1, 5, 6]. Several possible driving forces for particle rotations are identified:

- the desire to form low energy grain boundaries in the contact zones [7],
- asymmetric interparticle contact zones result in tension and
- inhomogeneous particle centre approach due to inhomogeneous packing of particles with differing particle sizes causing tensions.

In model experiments with particle rows, 2D arrangements of particles and observations of the surfaces showed, that cooperative material transport mechanisms occur. Especially at low temperatures and in specimens consisting of single crystal particles the contribution of rotations to the shrinkage can exceed 50 %. By combining the micro focus computed tomography (μ CT) with methods of photogrammetric image analyzing it becomes possible to measure rotation processes inside [8, 9] of 3D specimens and an extended database of experimental data will enable to improve existing computational simulations of sintering processes (e.g. [10, 11]).

Experiments

The in - depth analyzed specimens consisted of spherical air atomized copper powder (ECKA Granulate AK 0.1 - 0.125 mm). The powder was sieved to obtain 100...120 μm particles. The image analysis requires spherical particles. Thus the powder was rolled over a glass plate with an inclination angle of roughly 5° to separate spherical from other particles. The spherical particles were filled into aluminiumoxide crucibles of about 2.5 mm diameter. The specimen consisted of 9000...10000 particles as determined by photogrammetric image analyzing. The crucibles were marked with at least 6 notches as reference to obtain the precise voxel size. Micro focus computed tomography requires long data acquisition times and thus ex-situ measurements of the specimens. To fix the particles in their positions the specimens were sintered before the first analysis by μCT . The pre-sintering temperature was 600°C for the temperature series specimen and 1050°C in case of the time series specimen. After the μCT analysis of the pre-sintered specimens the next respective stage of sintering was prepared. Based on dilatometric experiments and prior operating experience following stages of sintering were prepared (pre-sintering included) and frozen in by rapid cooling to room temperature:

- 600, 700, 800, 900, 1000 and 1050°C with no dwell time for the analysis of the temperature series sample (referred as specimen 1)
- 1050°C with dwell times of 0, 5, 10, 20, 40, 80, 160 and 320 min during the respective preparation of a sintering stage of the time series specimen (referred as specimen 2).

The schematic drawing of the μCT setup is shown in figure 1. The acceleration voltage of the X-ray tube was set to 175 KV. The focal spot of negligible size on the tungsten transmission target emits bremsstrahlung, which was filtered by a 0.8 mm copper filter to optimize the image quality. The CCD camera obtains 1440 enlarged radiograms of the specimen with a resolution of 1024×1024 pixels. An additional beam hardening correction as described in detail in [8] was performed to ensure 3D data sets of optimal quality.

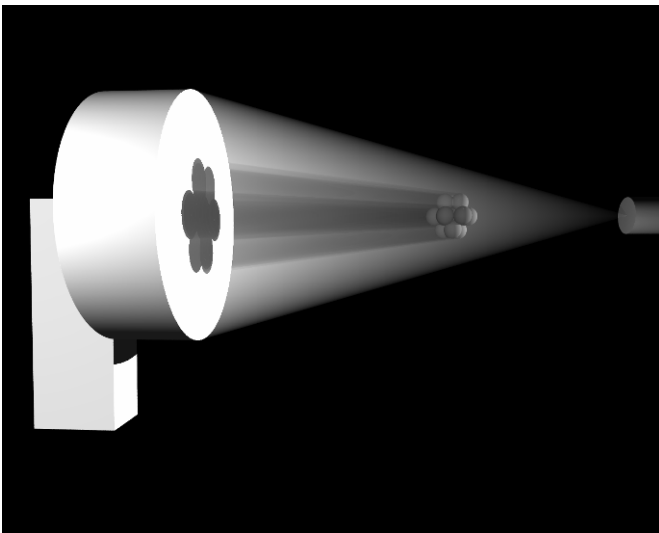


Fig. 1: Schematic drawing of the micro focus computer tomography setup

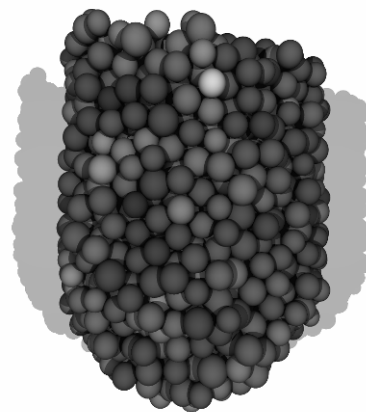


Fig. 2: 3D visualization of the temperature series specimen

Figure 2 shows a 3D visualization of the temperature series specimen based on the results of image analyzing. The edge particles and 4 subsequent particle layers are already removed. The grey value of the individual particles is set accordingly to the cumulated rotation at the particle positions.

Image analysis and statistical evaluation

The particle rearrangements during the sintering process were monitored by acquiring a time series of computer tomography data. Voxel - based photogrammetric image analysis techniques were used to derive geometrical and topological particle parameters automatically from multi - temporal voxel data. The process of automatic image analysing is divided in detection and modelling. At first the object of interest has to be found and identified in general. The focus in this part lies rather on the reliability of object detection instead of accuracy in position or shape. This step delivers just an approximation in object description. Based on this approximation the object will be modelled by using accurately operating subvoxel algorithms and methods to bring out its object surface and details. Because these operators base on many object parameters in advance the detection step has to provide a reliable base.

The original 3D data set is float type and has a dimension of 1024x1024x1024. Due to distortion correction and imperfection in placing the sample in the rotation axes the work dimension shrink to around 800x800x800. Typical for computer tomography the image is characterised by artefacts and noise effects. The average signal-to-noise-ratio is low at around 5/1 and the edge slip with 45 ° indicates a flat edge rise. With a resolution of 4.5 µm/voxel a sinter particle diameter is represented by about 22 voxels. To overcome the lack of resolution the use of subvoxel accuracy operators allow the determination of particle parameters with a precision of better than 1 µm.

The objects of interest are spherical copper particles with a diameter of around 22 voxels in the image. The algorithm indicates points which are surrounded by a sphere of homogeneous grey value above a certain minimum level as candidates of the object centre. To overcome the problem of describing all particles (around 10000) with the same set of parameters (search radius, grade of homogeneity, minimum grey value) an iterative approach was implemented. Starting with a very strict parameter definition and weaken more and more this configuration allows us to find nearly 100 % of the particles correctly. After each iteration the found objects are deleted in the image by setting their grey value to zero.

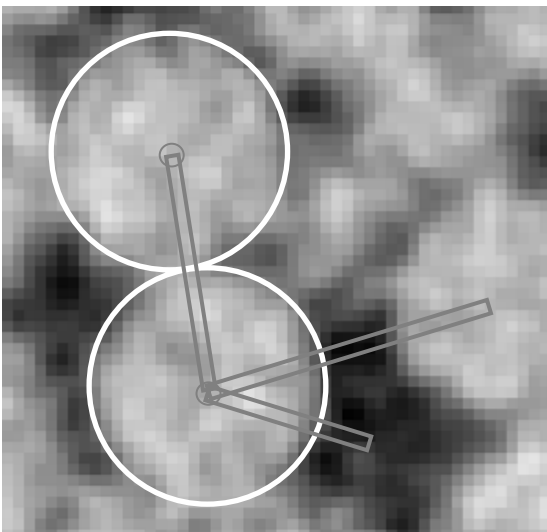


Fig. 3: Schematic drawing of the profile line measurement

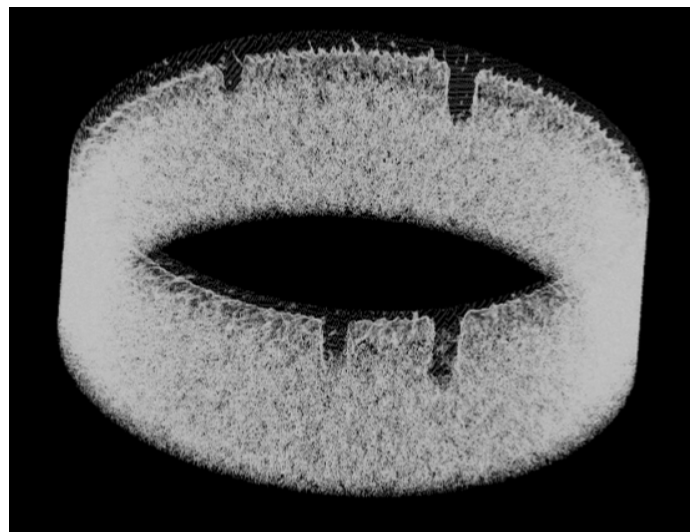


Fig. 4: Marked cuts in the crucible for the affine transformation

The located candidates are the starting point for the modelling step. By measuring profile lines from the approximated centre point to the outside and determining the maximum grey value difference an edge or surface point of the particle is found. In this way for every direction in space points on the object surface can be found. From these points the parameters of the selected geometrical model (sphere, ellipsoid etc.) can be estimated. Different geometrical models can be used to modelling the

particle. The sphere model the simplest abstraction describes a particle with four parameters. Particle constellation and particle motion parameters can be determined from the geometrical parameters. For the statistical evaluation beside the geometrical parameters topological parameters were needed to analyse the relation between neighbouring particles. The interparticle contact behaviour was determined by the total number of contact partners, new and broken contacts.

In order to compare the single step of a time series a 3D affine transformation on base of marked cuts in the crucible was calculated for all images. The average error in translation and rotation was less than $1\ \mu\text{m}$ or $1/10$ voxel. To track the sintering particle during the sintering process another transformation was used to model the rotation and shrinking effects of the whole sample in general. 30 homolog particles were used for that. The method to derive particle parameter from surface points assume that between the particles is enough free space to determine surface points. With increasing local density less points are available for the parameter estimation and the accuracy drops to $1/2$ voxel for the densest regions.

Based on the results of image analyzing various parameters were calculated. Based on the Voronoi tessellation of the dataset in relation to the particle volumes a density can be assigned to each particle. The rotation of a particle is measured by the change of angles in all triplets consisting of the particle itself with two coordinating particles. In addition changes of the coordination due to breaking and formation of interparticle contacts were determined. The contribution of the interparticle contact growth to the sintering process was determined by the distance to the next coordinating particle.

Effects inflicted by the edge particles were minimized during the data analysis. To achieve this all edge particles and all particles within a range of 4 particle diameters from the edge were excluded from the data analysis. If necessary the densities of the parameters were calculated. All particle centres within a sphere with a diameter of 2 to 8 particle diameters around the particle were determined (based on the local densities we estimate, that roughly 170 particles can be found within a sphere with a diameter of 8 particle diameters). The mean values of the parameters within the sphere yields the density of the parameter at the position of the central particle. In diagrams the parameters will be labeled as follows

1. O_x for cumulative values of differential parameters like rotation or number of new interparticle contacts or the value of the parameter in the pre-sintered specimen. Otherwise S for changes occurring during one sintering step of differential parameters or the value of the parameter in the first of both examined stages of sintering
2. E followed by a number required distance of a particle centre to the next edge particle for the inclusion in the statistical data analysis measured in particle radii
3. S followed by a number diameter of the sphere applied to calculate the parameter density

Results

Figure 5 shows the distance between next coordination partners plotted versus the relative density of both specimens. During the entire sintering process a densification is observed. At temperatures below $900\ ^\circ\text{C}$ the distance between coordinating particles obviously stays constant. At higher temperatures the temperature series specimen shows a particle centre approach. Similarly the time series specimen shows a continuous particle centre approach. It must be concluded, that the contribution of the particle centre approach – as described by the two particle model - to the densification of the specimens is negligible below $900\ ^\circ\text{C}$. The densification below this temperature must be attributed to the cooperative material transport. Simultaneously to the densification of the specimen a continuous increase of the coordination is observed. This and the observation of the breaking and formation of interparticle contacts also require the occurrence of particle rearrangements.

Figure 6 shows the differential rotation occurring in the time series specimen during the first and third sintering step. The differential rotations measured after the preparation of the third sintering stage at

900 °C give a good idea of the detection threshold for rotations. The increase of the detection threshold from roughly 0.9 ° in regions of low density to more than 1.5 ° in regions with high density is easily understandable. With increasing density the number of free surface points of the particles decreases and with that the accuracy of the measurement of the particle centres decreases. In regions with low local density of the temperature series specimen the differential rotation during the first sintering step obviously exceeds the values measured during the subsequent sintering steps. The time series specimen shows no significant differential rotations beyond the detection threshold

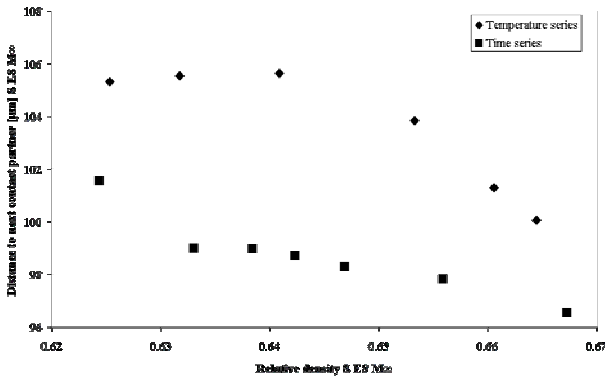


Fig. 5: Distance to next coordination partner vs. specimen density

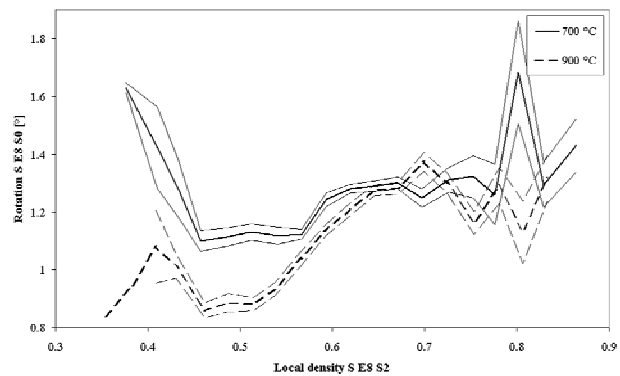


Fig. 6: Differential rotation of the temperature series sample vs. the local

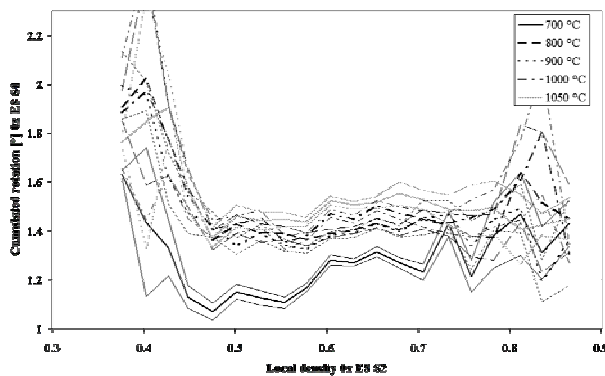


Fig. 7: Distance to next coordination partner vs. specimen density

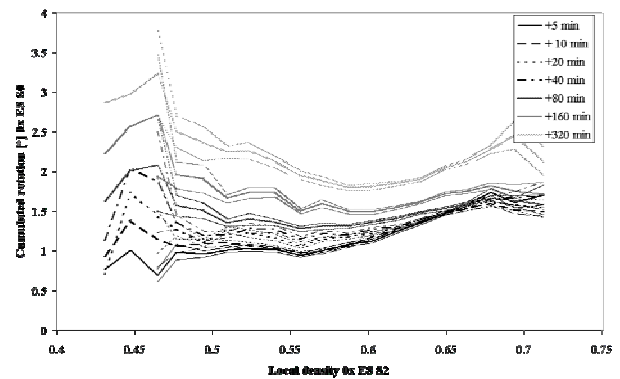


Fig. 8: Cumulated rotations in the time series specimen vs. local density

The cumulative rotations are more meaningful. The scatter bands of the cumulated rotations plotted versus the local densities of the temperature series specimen are shown in figure 7. Especially in regions with densities below 50 % a steep increase of the cumulated rotation is observed for all analyzed stages of sintering of the temperature series specimen. With increasing temperature the cumulated rotation increases until a temperature of 900 °C is reached. During the first sintering step with detectable particle centre approach a decrease of the cumulated rotation is observed. During the following sintering stages the cumulated rotation increases again. At the elevated temperatures the growth of accumulated rotations is most pronounced in regions of medium densities.

The scatter bands of the cumulated rotations plotted vs. the local densities of the time series specimen are shown in figure 8. Obviously a continuous rotation occurs. As already observed during the measurement of the temperature series specimen the most extensive rotations occur in regions with low local density.

Obviously in regions with low density the rotations due to the desire to form low energy grain boundaries occurred during the initial sintering steps. This yields a significant decrease of the remaining driving force. This is backed by the observation of the samples analyzed by dilatometry.

The samples showed extensive swelling after the pre-sintering step. Once a significant growth of particle contacts and with that a diversification of contact sizes begins the direction of rotation obviously often changes. As the interparticle contacts of one particle start to grow the balance of driving forces inflicted by the coordination partners can be tipped due to the diversification of the contacts. Particles in the optimal path of rotation have to be pushed away by the rotating particle. Consequently in regions with high density the rotations are inhibited. Thus in these regions the driving forces for rotations prevail longer than in regions with low density.

Conclusion

By combining Micro focus computed tomography with photogrammetric image analyzing it becomes possible to analyze particle rearrangements as well as the formation and breaking of interparticle contacts inside of 3D specimens. We could analyze specimens consisting of 100...120 μm spherical copper particles. Even at temperatures below the first detectable particle centre approach (under 900 °C) densifications of the specimen occurred. We have to conclude that this initial densification is caused by cooperative material transport processes. The most extensive rotations occur in regions with low local density. In these regions the inhibiting forces are smaller giving the opportunity for fast rotations. Once the inter particle contacts start to grow the balance of driving forces can change and even yield reverse rotations. As the sintering process proceeds the driving force for rotations only slowly decreasing in regions with high local density. Thus the difference of accumulated rotations between areas of low and high density can be slightly reduced as the sintering proceeds.

Acknowledgements

The authors would like to thank the DFG (Deutsche Forschungs Gemeinschaft) for the financial support of our research. Furthermore we are grateful to the ECKA Granulate GmbH & Co. KG for the supply of copper powder.

References

- [1] Geguzin, J.E.: Physik des Sinterns, VEB Deutscher Verlag für Grundstoffindustrie, Leipzig, 1973
- [2] Schatt, W.: Sintervorgänge, VDI-Verlag 1992
- [3] German, R.M., Sintering in theory and practice, John Wiley & Sons, Inc. 1996
- [4] Exner, H.E. Jahrbuch „Technische Keramik“, Essen (1988), Vulkan-Verlag, 28
- [5] Exner, H.E.; Grundlagen von Sintervorgängen. Berlin/Stuttgart: Gebrüder Borntraeger 1978
- [6] Wieters, K.P.: Korngrenzeneinfluß beim defektaktivierten Sintern; Dissertation B; TU Dresden 1989
- [7] Sutton, A.P., R.W. Balluffi, Interfaces in crystalline materials, Oxford University press (2003)
- [8] Nöthe, M., Pischang, K., Ponížil, P., Bernhardt, R., Kieback, B.: Advances in Powder Metallurgy & Particulate Materials - 2002, ISBN: 1-878954-90-3, Part 13, pp.176-184
- [9] Lame O., D. Bellet, M. Di Michiel, D. Bouvard, Nucl. Inst. And Meth. in Phys. Res. B 200 (2003) 287-294
- [10] Redanz, P. and R.M. McMeeking, Philosophical Magazine, Vol. 83, p. 2693 (2003).
- [11] Olevsky, E.A., Theory of sintering: from discrete to continuum, Mater. Sci. Eng. R23(1998), pp. 41-100